A decision support framework for the evaluation of installation strategies of superstructures for offshore wind farms

Frijlink, Tenzin; Fazi, Stefano; Tavasszy, Lori; Duinkerken, Mark; Lammers, Leon

DOI
10.1016/j.oceaneng.2025.121144

Publication date
2025

Document Version
Final published version

Published in
Ocean Engineering

Citation (APA)
Frijlink, T., Fazi, S., Tavasszy, L., Duinkerken, M., & Lammers, L. (2025). A decision support framework for the evaluation of installation strategies of superstructures for offshore wind farms. *Ocean Engineering*, *329*, Article 121144. https://doi.org/10.1016/j.oceaneng.2025.121144

Ocean Engineering 329 (2025) 121144

Contents lists available at ScienceDirect

Ocean Engineering

journal homepage: www.elsevier.com/locate/oceaneng

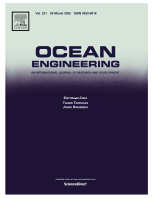

Research paper

A decision support framework for the evaluation of installation strategies of superstructures for offshore wind farms

Tenzin Frijlink [a], Stefano Fazi [b,*], Lori Tavasszy [b], Mark Duinkerken [c], Leon Lammers [d]

[a] Delft University of Technology, Faculty of Civil Engineering, the Netherlands
[b] Delft University of Technology, Department of Technology, Policy and Management, P.O. Box 5015, 2600 GA, Delft, the Netherlands
[c] Delft University of Technology, Faculty of Mechanical Engineering, the Netherlands
[d] Royal HaskoningDHV, the Netherlands

ARTICLE INFO

Keywords:
Offshore wind energy
Transportation and installation
Wind turbines
Simulation
Optimization
Shuttling
Feedering
Manufacturing ports

ABSTRACT

The demand for new offshore wind farms is increasing at a rapid pace, and the installation rate must be quadrupled by 2030 to meet the ambitions of European countries. The installation of the superstructures involves several components and is highly weather-dependent, making this an important bottleneck. In this paper, we evaluate the two main strategies for the installation of superstructures: feedering and shuttling. With feedering, the installation vessel is fed with components by feeder vessels directly from manufacturing ports. With shuttling, the installation vessel retrieves the components itself from a marshalling port. In contrast to existing studies, we include manufacturing ports and their production rate to have a better understanding of their influence on the installation rate and develop a rolling horizon optimization-simulation framework composed of a mixed integer linear programming model and a Markov simulation model for weather forecasting. A heuristic is proposed to solve the model to overcome the limitation of commercial solvers. Results indicate that accurate initial buffer calculations, depending on the production rate at the manufacturing ports and project-dependent characteristics, can increase the installation rate significantly for both strategies. Finally, feedering outperforms shuttling in most scenarios and is less weather dependent.

1. Introduction

European countries surrounding the North Seas have set a goal of installing at least 120 gigawatts (GW) of offshore wind energy by 2030 (NSEC, 2023). Currently, only 30 GW is currently installed, which means a fourfold scale-up is required in the upcoming years. However, this scale-up is faced with many challenges, such as a limited fleet of Wind Turbine Installation Vessels (WTIVs), bottlenecks in port capacity, and weather-dependency of operations (uit het Broek et al., 2019; CEIF, 2022). Hence, more and more studies on the installation logistics have been conducted (Tjaberings et al., 2022). Within the total costs for offshore wind farms (OWFs), the transportation and installation stage makes up 20 % of the total costs (Sarker and Faiz, 2017). Additionally, weather-related delays during installation account for over 20 % of the time required for offshore wind projects (Lerche et al., 2022). Barlow et al. (2015) indicate loading operations also contribute significantly to the total delay, making the transportation and installation of offshore wind farms relevant from a cost and time perspective.

In this paper, we focus on superstructure installation for wind turbines, referring to the installation of the tower, the nacelle, and three blades by the WTIV. Compared to substructure installation (i.e., the foundation of the wind turbine), it involves more components and is more weather-sensitive (Rippel et al., 2019b). We explore two installation strategies: shuttling and feedering. Fig. 1 illustrates the difference in the logistics between these two strategies. Rectangles indicate physical locations, whereas rounded rectangles indicate which vessels are required for transportation or transshipment. With shuttling, the WTIV collects components itself at a marshalling port, and with feedering, the WTIV remains offshore and gets supplied directly via feeder vessels from the manufacturing ports. The risk of shuttling is that the WTIV spends more time sailing than installing, whereas, for feedering, the risk is that there are insufficient weather conditions for both transshipping and installing offshore. Additionally, the location of and production rate of components at the manufacturing ports are of great importance to installation efficiency and may severely impact the installation time (Hrouga and Bostel, 2021).

Literature on the superstructure installation phase of wind turbines has increased in the past few years due to the increasing size of wind farms, wind turbines required installation capacity, and costs (Ren et al., 2018). Existing studies show several limitations. In Rippel et al. (2019b)

* Corresponding author.
E-mail address: s.fazi@tudelft.nl (S. Fazi).

https://doi.org/10.1016/j.oceaneng.2025.121144
Received 28 October 2024; Received in revised form 7 March 2025; Accepted 1 April 2025
Available online 8 April 2025

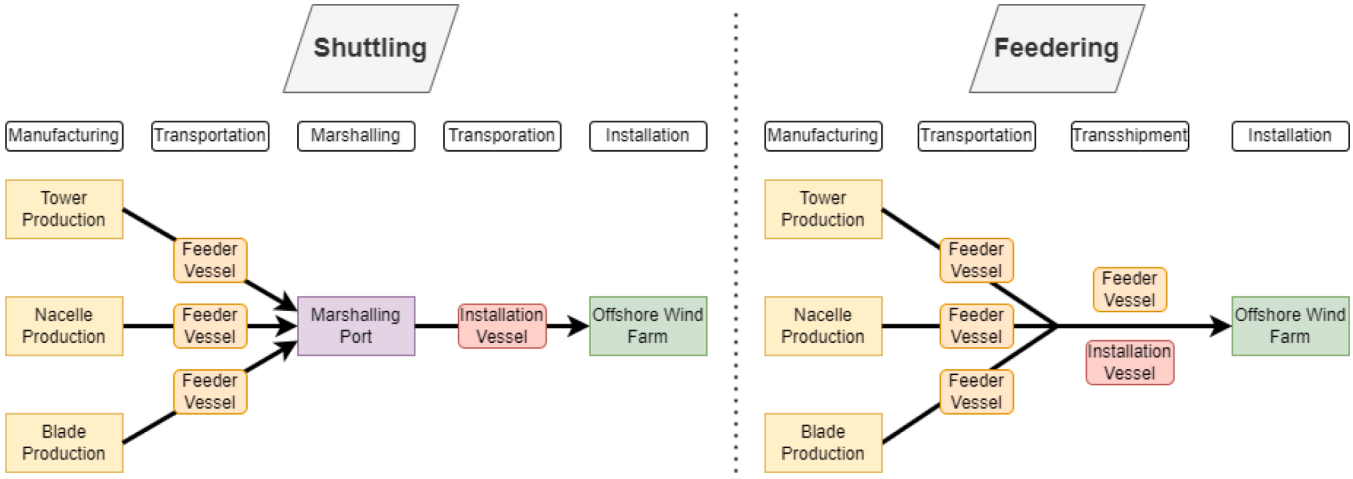

Fig. 1. Shuttling and feedering logistics respectively.

and Irawan et al. (2017), only shuttling is considered, but interesting optimization and simulation methods are used. In Tjaberings et al. (2022), feedering is considered, but for the installation of substructures and without considering manufacturing ports. The closer work to our study is the conference paper of Oelker et al. (2018) that compares shuttling and feedering but uses historical weather data and does not consider the production rate at manufacturing ports. Moreover, we provide a more accurate forecasting tool based on Markov chains to best capture stochasticity in weather conditions.

The goal of this paper is to develop a comprehensive framework to analyze superstructure installation strategies for offshore wind farms considering the production rate of components. The paper makes four contributions to the literature. Firstly, our study combines shuttling, feedering, manufacturing ports, port capacity and forecasted weather in a dynamic modeling framework. We develop a rolling horizon optimization-simulation framework composed of a mixed integer linear programming model and a Markov simulation model for weather forecasting. Secondly, a tailored heuristic is proposed to overcome the limitation of commercial solvers to solve instances quickly. Thirdly, by means of a set of case studies from the North Sea, we analyze key factors for each strategy, such as port locations, buffer size, and vessel size. The numerical experiments using real-world data show the benefit of the strategies and how project-dependent nuances can affect the results. Fourthly, we arrive at the new result that under most scenarios, feedering is preferred over shuttling. Only in a limited number of specific cases, shuttling performs better.

This paper is structured as follows. In Section 2, we provide a review of relevant literature. In Section 3 we provide a formal definition of the problem along with the decision support framework. Section 4 we show the numerical tests to analyze the different strategies and provide a comprehensive sensitivity analysis based on real-world data. Sections 5 and 6 concludes our paper with a discussion and synthesis of the results respectively.

2. Related work

Installing a wind turbine entails the positioning and installation of the substructure as well as the superstructure. Afterward, the substation is installed, which collects the cables from all wind turbines and connects them to the shore. All these structures are installed independently, as structure-specific vessels are required, so it is considered not a relevant simplification to focus on a specific stage (Rippel et al., 2019a). Superstructure installation, also called wind turbine installation, is the most complex transportation and installation stage, as it requires several sequential weather-dependent installation operations compared to substructure installation (Rippel et al., 2019b). Also, the number and type of components (in terms of size and weight) are quite different, making it necessary to evaluate these two stages apart. The interested readers are referred to Vis and Ursavas (2016) or Rippel et al. (2019a) for literature reviews on superstructure installation and to Hong et al. (2024) for a review specific on floating offshore wind farms. To our knowledge, no such review exists for substructure installation, but we refer to Tjaberings et al. (2022) for one of the most recent works. For a framework on the high-level logistical decisions, such as port and vessel selection, refer to the recent work of (Gonzalez et al., 2024).

The number of studies on superstructure installation has increased in recent years. The following studies focus on shuttling, as it is the standard strategy in practice. One of the first optimization attempts was the work of Scholz-Reiter et al. (2010), who used a MILP to find short-term schedules while considering different weather scenarios, installation concepts, and load capacities. However, the scheduling problem is NP-hard, so the MILP was only able to solve small scenarios. Consequently, they later developed a heuristic to solve larger instances and longer planning periods (Scholz-Reiter et al., 2011). Irawan et al. (2017) developed a bi-objective optimization model, which tries to balance project duration and costs. Their metaheuristic method, which includes greedy heuristics, performed well and is much faster than the exact method. Rippel et al. (2019b) stated that resource restrictions at the port and uncertainty in weather predictions are often neglected. Therefore, they proposed a Mixed-Integer Linear Programming (MILP) for the scheduling in combination with a Markov model to forecast weather conditions. They find that the installation efficiency and port usage strongly depend on the weather conditions. Ursavas (2017) used Benders decomposition and also highlighted the uncertainty with regard to weather conditions. The results showed that including weather uncertainty can reduce the project duration and increase the installation rate compared to typical planning approaches that use historical weather data. Barlow et al. (2018) developed a mixed method with both simulation and optimization. Simulation allows developers to make long-term strategic decisions, whereas optimization can provide robust schedules.

Oelker et al. (2018) compared feedering and shuttling, using a discrete-event simulation model to test the performance of either strategy under different conditions, such as distance to the wind farm and fleet size. Feedering generally performs better than shuttling, except if the distance to the wind farm is too large or the fleet of feeder vessels is too small. However, their study did not consider manufacturing ports and port capacity. Quandt et al. (2017) considered port capacity, i.e., the available storage space, via simulation and found that efficient utilization of the port capacity significantly improves the installation rate. Similarly, Oelker et al. (2020) found that due to the increasing size of wind turbines and projects, the concept of shuttling might not be feasible in the future due to the limited port capacity. Beinke et al. (2017) took a

Table 1
Overview of reviewed T&I literature.

Author	Sim	Math	Weather	Shuttling	Feeder	Manu	Port cap.
Beinke et al. (2017)	✓		✓	✓		✓	
Irawan et al. (2017)		✓	✓	✓			
Quandt et al. (2017)	✓		✓	✓		✓	✓
Ursavas (2017)		✓	✓	✓			
Barlow et al. (2018)	✓	✓	✓	✓			
Oelker et al. (2018)	✓		✓	✓	✓	✓	
Rippel et al. (2019b)	✓	✓	✓	✓			
Oelker et al. (2020)	✓		✓	✓			✓
Tjaberings et al. (2022)	✓		✓	✓	✓		
This paper	✓	✓	✓	✓	✓	✓	✓

more supply chain-oriented simulation approach and found that including additional aspects, such as manufacturing ports, can lead to more insights into the mutual effects of different parts of the logistical system and thus increase installation efficiency. Paterson et al. (2018) assess the impact of vessel technology on construction durations for offshore wind farms to evaluate the installation durations through simulation.

There are three main takeaways from the reviewed literature. Firstly, only two papers consider feedering as a transportation strategy. Secondly, only three papers consider manufacturing ports. Moreover, these papers assume production times are sufficiently fast to always have components available. Thirdly, only two papers take into account port capacity, while this is a significant bottleneck and could limit project duration significantly (NSEC, 2023). From Table 1, it becomes clear that this paper is the first to address feedering, manufacturing ports, and port capacity simultaneously. Our literature review is synthesized in Table 1.

3. Methodology

First, Section 3.1 describes the rolling horizon modelling approach. Next, the Markov weather simulation model is detailed in Sections 3.2 and 3.3 describes the optimization model. Lastly, Section 3.4 describes how the updating process is performed.

3.1. Rolling horizon modelling approach

The complexity of the problem in this paper lies in the dynamic nature of weather conditions, which can only be reliably forecasted for roughly two weeks (Ritchie, 2024). Hence, a rolling horizon approach is a valid option to solve the problem at hand. Similarly to Rippel et al. (2019b), we use a simulation loop where weather conditions are dynamically forecasted, and based on these predictions, the optimization model is launched. At the same time, the actual weather conditions are realized, and based on these, the input for the optimization model is updated.

In short, three steps can be distinguished. First, the weather forecast estimates the duration of all vessel actions through simulation. Second, an optimization model is used to create a vessel schedule based on these action durations for a given forecast period. Third, the system state is updated, i.e. actions are performed for the current time step, and the model moves to the next time step. This process is repeated until some stopping criterion is met (e.g., all turbines are installed). At the beginning of this approach, the system is initialized, following the current vessel and port states and the time is set to zero (Fig. 2).

3.2. Markov weather simulation model

Markov models are a commonly used approach to produce weather forecasts (Pandit et al., 2020). Whilst the general Markov principle is quite simple, some important considerations for implementation can influence the performance significantly. Capturing seasonality is one such consideration. If one probability matrix is used for all forecasts, there is no variation over the year. Thus, forecasts during summer will not be different from forecasts during winter. Therefore, to realistically capture seasonality trends, monthly probability matrices are used, similar to Pandit et al. (2020).

Additionally, Pandit et al. (2020) find a strong correlation between wave height and wind speed. This was confirmed by the weather data available in this research, with correlations of over 0.85 between wind speed and wave height. With the operational limits of this report, the wave height is only necessary for the jacking operations of the WTIV and transshipment, whereas the wind speed is needed for every weather-dependent operation. Moreover, Ursavas (2017) states that wind speed is the limiting factor for the operational limits, not wave height. Therefore, only wind speeds are forecasted, and then the wave height is determined based on the correlation between wave height and wind speed using a simple linear regression model with intercept and coefficient.

Another important consideration for the implementation of Markov models is the number of weather states. If too many states are considered, no historical transitions could be available or the model could become very large. On the other hand, if too few are considered, the states may not represent reality sufficiently. Therefore, for this report, the number of considered weather states are integer values of wind speed in m/s from 0 to the maximum value recorded in the available data set. This strikes a good balance in terms of aggregation and fully captures the operational limits, which are also in integer m/s.

A parametrized approach is proposed to determine action durations. To determine appropriate action durations, N simulations are performed where each simulation represents a singular forecast. Then a safety benchmark, ρ, which is a fraction of the simulation is used as follows. If in fraction ρ of the simulations the activity can be completed within D time units, this is the time duration of that operation for the optimization model, where D is as low as possible.

3.3. Optimization model

The optimization model is used to create a vessel schedule based on these action durations for a given forecast period. Section 3.3.1 motivates the use of a network flow model and provides the mathematical

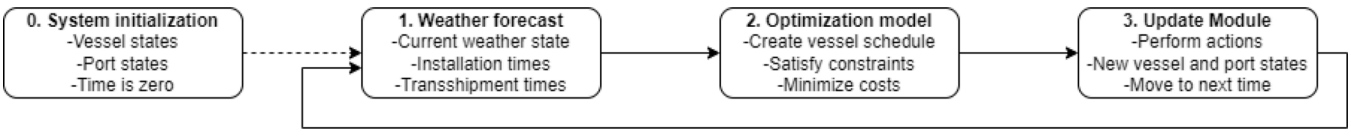

Fig. 2. Overview of the rolling horizon approach.

model and assumptions. Furthermore, Section 3.3.2 provides a heuristic approach to solve this MILP.

3.3.1. Mathematical model

To model the problem mathematically, we use a network flow representation. There are three basic operational stages: manufacturing, transportation, and installation. The manufacturing and installation stages are represented as single steps, but all operational steps of feedering and shuttling are kept in detail. This approach strikes a balance by simplifying independent operations but retaining the complexity associated with the transportation strategies and thus captures the essence of the problem. A network flow model is a logical choice for the model, as there is a natural component flow from the manufacturing ports to the offshore wind farm Tian et al. (2023). An example is provided for shuttling in Fig. 3 and feedering in Fig. 4.

We endow the network flow model with five features. First, discrete time steps are introduced to allow for the inclusion of weather conditions. Second, multiple commodities are introduced to represent the different components required for installation. Third, dummy nodes are introduced for each feeder vessel to model the choice of one of them for transportation (see in both figures that nodes 6 and 7 are the dummy nodes of the two available feeder vessels). Fourth, for the shuttling strategy, we define a return arc from the OWF to the marshalling port for the WTIV because it can be decided that the WTIV returns to the marshalling port before all components on board are installed if the weather conditions worsen (see the arc from node 10 to node 9 in Fig. 3). Finally, the transshipment activity in the feedering strategy requires both the installation vessel and feeder vessel to be available at the same time, implying that synchronization constraints are needed.

The mathematical formulation is inspired by the model in Tian et al. (2023). Although their study focuses on a different application, namely resource-constrained project scheduling and material ordering, we convert their formulation into a suitable form for wind farm installation, including manufacturing ports and production rates. In addition, we add synchronization between the resources for transshipment operations.

We define a directed graph $G = (V, A)$ with nodes $i \in V$ and arcs $(i, j) \in A$. Each node of the network is defined for every discrete time $t \in T$. We also define the set of components $k \in K$ to be installed. Next, we consider the following subsets of A: A_i^{Dep} indicating the dependent

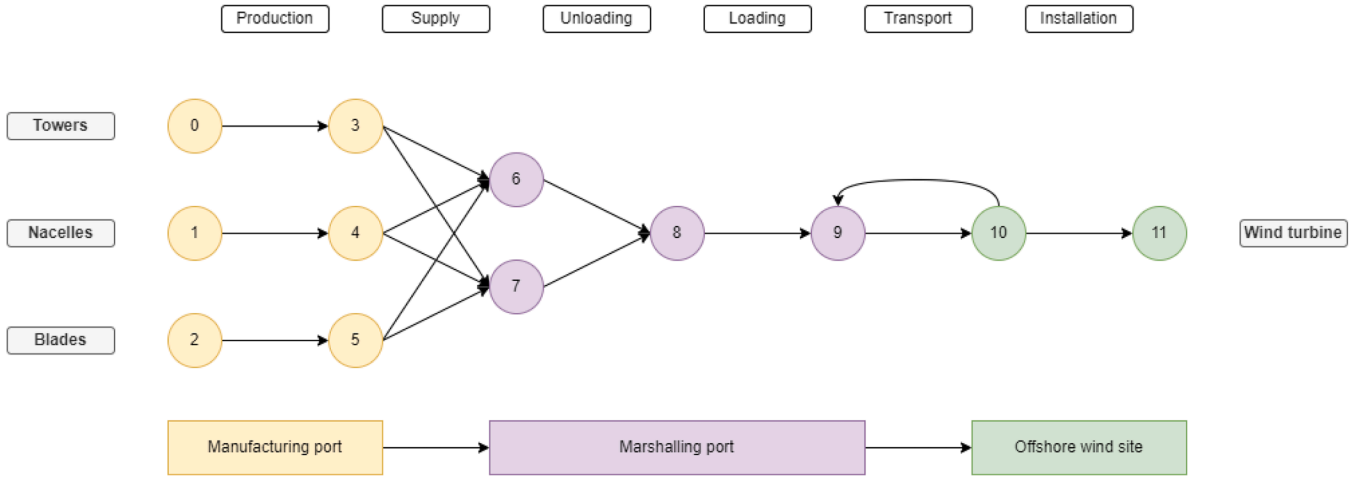

Fig. 3. Network flow representation of shuttling with two feeder vessels. Activities are indicated at the top, and the colour of the nodes indicates the physical locations.

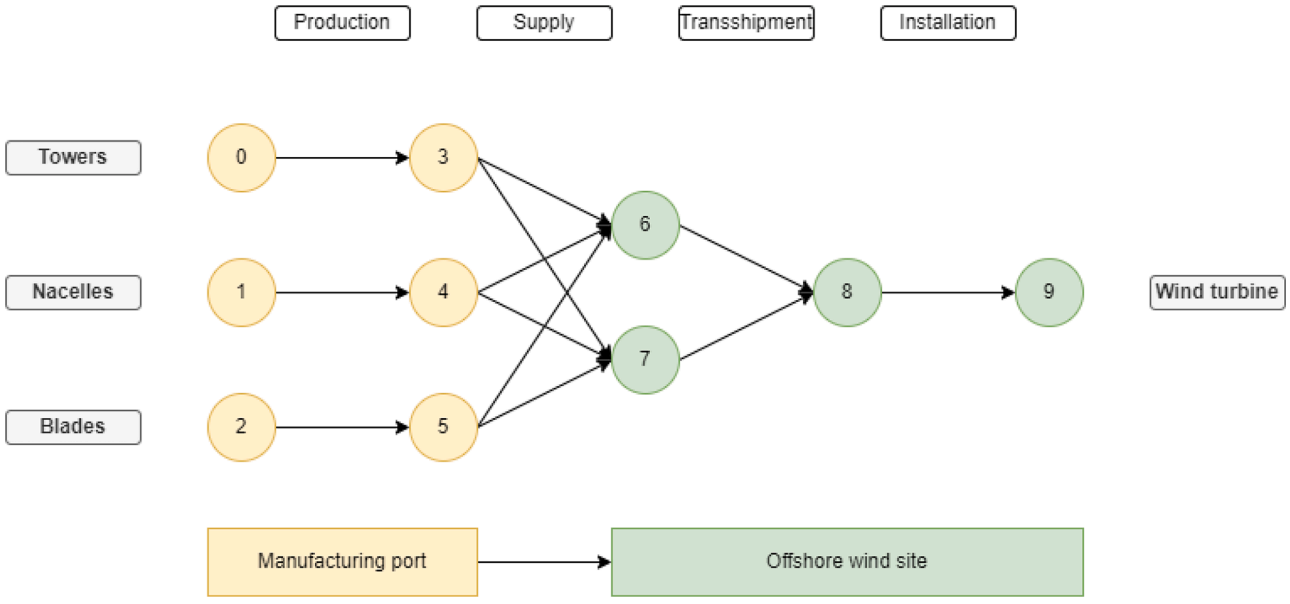

Fig. 4. Network flow representation of feedering with two feeder vessels. Activities are indicated at the top, and the color of the nodes indicates physical locations.

nodes for node i, A_{ij}^{Dep} indicating the dependent arcs for arc (i,j), A^{Inst} indicating the installation arc(s) and A^{Trans} indicating the transportation arc(s). Lastly, with $F_+(i^t)$ and $F^-(i^t)$ which we indicate the in- and outgoing arcs of node i at time t respectively.

Let us consider C_{ij}^t, the cost to use arc (i,j) at time t and C_i, the inventory costs per area per time period at node i. Next, D_{ij}^t indicates the duration arc (i,j) is in use when starting at t. It should be noted that D_{ij}^t is used to capture the production rates as well as varying vessel speeds and durations of weather dependant operations. Since D_{ij}^t is defined per time period, different durations can be applied for different time steps, thus allowing us to capture the stochasticity of weather conditions. Moreover, each arc can have a different duration, thus allowing for varying vessels speeds and production rates per arc. For each arc, we define a transfer capacity U_{ij}^k per component, and for each physical node (e.g., ports), the available storage area is L_i, where a component k takes up S^k of it. Additionally, P_k indicates how many components are required for installation, and Q_i^k indicates how many components are available initially. Finally, M is a sufficiently large number.

There are two decision variables per arc, namely x_{ij}^{kt} and y_{ij}^t, where x_{ij}^{kt} indicates the integer flow of components k on arc (i,j) at the start of time period t, and y_{ij}^t is a binary variable that indicates if the arc is activated in time period t. The other decision variable is b_i^{kt}, which indicates the integer inventory of component k at node i at the end of time period t.

The mixed integer linear programming model is defined as follows:

$$\min \sum_{t\in T}\left(\sum_{(i,j)\in A} C_{ij}^t y_{ij}^t + \sum_{i\in V}\sum_{k\in K} C_i b_i^{kt}\right) \tag{1}$$

$$M * y_{ij}^t \geq \sum_{k\in K} x_{ij}^{kt} \qquad \forall (i,j)\in A, \forall t \in T \tag{2}$$

$$\sum_{z=t+1}^{z=\min T, t+D_{ij}^t} y_{ij}^z \leq 1 - y_{ij}^t \qquad \forall (i,j)\in A, \forall t \in T^{-1} \tag{3}$$

$$\sum_{(m,l)\in A_{ij}^{Dep}} \sum_{z=t}^{z=\min|T|, t+D_{ij}^t} y_{ml}^z \leq (1 - y_{ij}^t) * M \qquad \forall (i,j)\in A, \forall t \in T \tag{4}$$

$$b_i^{k,t+1} = b_i^{kt} + \sum_{(j,i)^z\in F^+(i^{t+1})} x_{ji}^{k,z} - \sum_{(i,j)^z\in F^-(i^{t+1})} x_{ij}^{k,z} \qquad \forall i \in V, \forall k \in K, \forall t \in T \setminus t^{max} \tag{5}$$

$$x_{ij}^{kt} \leq U_{ij}^k \qquad \forall (i,j)\in A\ , \forall k \in K, \forall t \in T \tag{6}$$

$$\sum_{k\in K} b_i^{kt} * S^k \leq L_i \qquad \forall i \in V, \forall t \in T \tag{7}$$

$$\sum_{k\in K} b_i^{kt} \leq \left(1 - \sum_{(m,l)\in A_i^{Dep}} y_{ml}^{t+1}\right) * M \qquad \forall i \in V, \forall t \in T \tag{8}$$

$$x_{ij}^{kt} P^k = y_{ij}^t \qquad \forall (i,j)\in A^{Inst}, \forall k \in K, \forall t \in T \setminus t^{max} \tag{9}$$

$$b_i^{k0} = q_i^k \qquad \forall i \in V, \forall k \in K \tag{10}$$

$$\sum_{z=0}^{z=t} y_{ij}^z \leq \sum_{z=0}^{z=t} y_{ji}^z + 1 \qquad \forall (i,j)\in A^{Trans}, \forall t \in T \tag{11}$$

$$\sum_{z=0}^{z=t} y_{ji}^z \leq \sum_{z=0}^{z=t} y_{ij}^z \qquad \forall (i,j)\in A^{Trans}, \forall t \in T \tag{12}$$

$$x_{ij}^{kt} \in Z^+ \qquad \forall (i,j)\in A\ , \forall k \in K, \forall t \in T \tag{13}$$

$$x_{ij}^{kt} \leq U_{ij}^k \qquad \forall (i,j)\in A\ , \forall k \in K, \forall t \in T \tag{14}$$

$$b_i^t \in Z^+ \qquad \forall i \in V\ , \forall t \in T \tag{15}$$

$$y_{ij}^t \in \{0,1\} \qquad \forall (i,j)\in A\ , \forall t \in T\ , k \in K \tag{16}$$

The objective function (1), aims to minimize the total activity and holding costs. Constraint (2) ensures that if there is a flow of components, the arc must be used. Constraint (3) ensures that if the arc gets used at time t, it is unavailable for duration D_{ij}^t. Constraint (4) ensures a vessel can only traverse one arc simultaneously. Constraint (5) ensures flow conservation and constraint (6) the arc capacity. Constraint (7) keeps track of port inventory capacity and constraint (8) of offshore vessel inventory, which is only possible if the vessel is offshore. Constraint (9) ensures the correct components are used for installation. Constraint (10): initializes the inventory. Constraint (11) and (12) ensures the WTIV shuttles between the OWF and marshalling port for shuttling. Constraints (13), (14), (15) ensure non-negative integer variables and constraint (16) the binary variables.

In this model, we make four main assumptions. First, that non-weather-dependent processes can not be halted midway through an operation, e.g. it is not possible to stop manufacturing halfway through the process. Second, we assume a limited non-homogeneous vessel fleet is available, in terms of capacity and sailing speed, as is the case in practice. The model can capture this variation implicitly, via the activity duration and arc capacity, and as such captures reality. Third, we do not consider port congestion. Whilst it would be possible to adjust the model to include a limited number of berths at a port, this is not the main interest of this study and and as such is not considered. Fourth, we assume vessels can remain offshore indefinitely. Consequently, the installation vessel can remain offshore under all weather conditions without having to refuel or renew the crew, which especially impacts feedering. Normally, refuelling, recrewing or storms could be reasons to return to port. But it is estimated the frequency of recrewing or refuelling is low enough to not impact the results. During storms, no installation is possible regardless, which is why remaining offshore during storms is also not expected to impact the results significantly.

3.3.2. Heuristic for solving the MILP

The solution space of the proposed model is relatively limited since it is heavily constrained and is used in a rolling horizon approach with a limited time frame. However, a preliminary analysis showed that commercial solvers yet struggle to solve sufficiently fast for relevant instance sizes, also given the high number of repetitions required in the rolling-horizon loop. Metaheuristic approaches such as genetic algorithms or simulated annealing can be overly complex and could require different parametrizations to perform well (Fazi et al., 2015). Consequently, we develop an efficient tailored heuristic as a trade-off between runtime and solution quality. This should reduce the runtime while having a marginal effect on the solution quality since we use problem-specific characteristics. When building the solution, the heuristic aims to process the components as quickly as possible. Three steps can be distinguished per iteration: (i) Initialization, (ii) Solution generation (iii) Selection and update.

In the initialization (i), the current system state is used as the initial solution. This could result in certain vessels already operating. Therefore, at the start of the iteration, it is known for each arc whether or not it is active and for how long it will be unavailable if active. For this purpose, a new binary parameter is introduced: Y_{ij}^t, which indicates whether arc (i,j) is available at time t, 1 if so. If an arc is not available also the other dependent arcs are set with $Y = 0$. In this way, Y makes sure that difficult constraints about arc availability and time restrictions, such as (3), (4), and (11), are met.

Next, the algorithm performs a greedy choice (ii). The basic principle is that as many arcs as possible are activated since this should result in the highest flow of components through the network and, consequently, the highest installation rate. For the decision on which arcs should be activated, we generate n lists with different arc orderings to obtain n solutions. Given a certain list, the algorithm tries to activate the arcs in the list sequentially. The first list follows the natural order of the network: manufacturing arcs first and the installation arc last. The second list adopts the reversed order. Next, $\frac{n}{2} - 2$ lists are generated based on random orderings to diversify the search space and avoid local optima. Finally, the last $\frac{n}{2}$ lists are also based on random orderings; however,

arcs related to the WTIV are prioritized, to stimulate installation. For feedering, if the WTIV has sufficient components, the installation arc is prioritized. If it is missing certain components, the transshipment arcs are prioritized. For shuttling, if the WTIV is offshore and has sufficient components, the installation arc is prioritized. If not, the return arc is prioritized. After the n solutions are generated, the best one in terms of objective value is chosen. Finally, the algorithm implements the solution and updates the status of the network.

Overall this algorithm aims to exploit problem-specific considerations to effectively construct a good solution. This is done by smartly incorporating difficult constraints and only checking for simple constraints. Specific ordering sets are used to improve the performance and ensure the algorithm does not get stuck in local optima.

3.4. Update module

It is known where vessels are located and whether or not they are performing an action. If an action, which is currently ongoing, is unable to be finished due to bad actual weather conditions, this action is stopped. This does result in undesirable situations where vessels are sitting idle since another vessel could not finish its operation. Due to the stochastic nature of weather conditions, this does represent reality, where this is also not certain in advance. To implement these actions, some adjustments to the mathematical formulation were also needed. Besides each node having a starting inventory as in (10), each arc now also has a starting state and inventory as in (17) and (18). For (11) and (12) an additional binary parameter *inport* was added for the current location, which is 1 if the vessel is in port, which results in (19) and (20) respectively.

$$y_{ij}^{0} = y_{ij}^{ini} \qquad \forall (i,j) \in A \quad (17)$$

$$x_{ij}^{k0} = x_{ij}^{k,ini} \qquad \forall (i,j) \in A, \forall k \in K \quad (18)$$

$$\sum_{z=0}^{z=t} y_{ij}^{z} \leq \sum_{z=0}^{z=t} y_{ji}^{z} + 1 - inport \qquad \forall (i,j) \in A^{Trans}, \forall t \in T \quad (19)$$

$$\sum_{z=0}^{z=t} y_{ji}^{z} \leq \sum_{z=0}^{z=t} y_{ij}^{z} + inport \qquad \forall (i,j) \in A^{Trans}, \forall t \in T \quad (20)$$

4. Computational experiments

This section describes the case studies, experimental setup and numerical results. All tests are performed on a 2.8 GHz Intel Core i7-7700HQ Quad-Core processor. The algorithms are coded in Python and run with Visual Studio Code.

4.1. Case studies

Three reference projects are available: a finished project (NL) to validate the model, a current project (DE), and a future project (DK). These projects are summarized in Table 2, and locations are visualized in Fig. 5. Díaz and Guedes Soares (2020) find that wind farm dimensions and the capacity of the turbines are increasing rapidly. Therefore, this combination of projects allows for a reliable and realistic synthesis of results and was validated by industry experts. For an overview of ports used in the industry, refer to NSEC (2023), and for vessels, refer to H-Blix (2022).

For all projects, the feedering is hypothetical, as it is currently not applied. For DE and DK, ports and vessels are arbitrarily picked since the installation of the superstructures has not started yet. Turbine size and WTIV for DE and DK are chosen such that they represent current and future projects, respectively. Distances are calculated using the MIT maritime scgraph python package (Makowski, 2023). Table 3 shows the impact of turbine size on the vessel capacity and required storage area. The storage area for 15 MW turbines is based on NSEC (2023); the rest is estimated based on the 15 MW turbines and validated with industry experts.

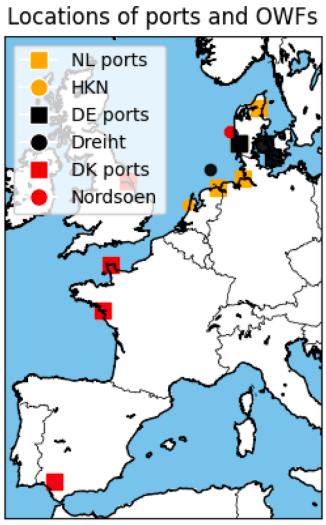

Fig. 5. Overview of project locations, squares indicate ports, circles indicate the OWF.

Table 2
Overview of reference projects.

OWF	NL	DE	DK
Name	HKN	Dreiht	Nordsoen
Size	0.69 GW*	0.96 GW	1.00 GW
WT size	10 MW*	15 MW	20 MW
Turbines	69	64	50
Ports	**NL**	**DE**	**DK**
Marshalling	Eemshaven	Esbjerg	Hull
Tower	Esbjerg	Esbjerg	Sevilla
Nacelle	Cuxhaven	Odense	St.-Nazaire
Blade	Aalborg	Nakskov	Cherbourg
Vessels	**NL**	**DE**	**DK**
WTIV	Small	Medium	Large
WTIV speed	10.5 kn	10.5 kn	10.5 kn
FV size	Medium	Medium	Medium
FVs	3	3	3
FV speed	14 kn	14 kn	14 kn

Note. In bold it is highlighted which project characteristic is summarized. i.e. OWF, Ports or Vessels for each of the reference projects (NL, DE, DK).

Table 3
Vessel capacity and storage space required per wind turbine size.

Vessel capacity	10 MW	15 MW	20 MW	Unit
Small	[3, 3, 9]	[2, 2, 6]	[1, 1, 3]	[Tower, Nacelle, Blade]
Medium	[5, 5, 15]	[3, 3, 9]	[2, 2, 6]	[Tower, Nacelle, Blade]
Large	[10, 10, 30]	[7, 7, 21]	[5, 5, 15]	[Tower, Nacelle, Blade]
Storage space	**10 MW**	**15 MW**	**20 MW**	**Unit**
Tower	0.07	0.1	0.15	ha
Nacelle	0.03	0.04	0.05	ha
Blade	0.05	0.07	0.1	ha

Note. Vessel capacity and storage space required depending on the turbine size.

Table 3 indicates how many sets of turbines a vessel can carry, so 3 indicates 3 towers, 3 nacelles and 9 blades, FVs only carry one component type since the manufacturing ports are dedicated to a single component. Besides the vessel and port capacities, weather dependency is one of the key challenges of this paper. Table 4 shows an overview of operations, based on installation, from Rippel et al. (2019b) and transshipment limits from Vis and Ursavas (2016).

In practice, operations are only allowed to happen sequentially, so if the wind speed is too high for a specific operation at any point during operations, that operation is not considered possible. Moreover, often a safety factor α is applied to the duration of the operation, as can be found in the industry guideline DNVGL-ST-N001.

Table 4
Overview of duration and operational conditions of relevant operations.

Operation	Duration (h)	Max. wind (m/s)	Max. wave (m)
(Un)load component (LC)	3	–	–
Transship component (TS)	3	12	2
Jack-up (JU)	3	14	2
Install tower (IT)	3	12	–
Install nacelle (IN)	3	12	–
Install blade (IB)	3	10	–
Jack-down (JD)	3	14	2

Note. "Operation" shows the operation. "Duration" shows the duration of that operation and "Max. Wind" and "Max. Wave" show the maximum allowed wind speed and wave height respectively, – means no limit. Units are indicated in brackets.

Table 5
Estimates of essential costs for ports and vessels.

Ports	Unit	10 MW	15 MW	20 MW
Handling	Per lift	€5,000.00	€8,000.00	€11,000.00
Holding	Per m^2/year	€100.00	€100.00	€100.00
Vessel	**Unit**	**Small**	**Medium**	**Large**
FV	Per day	€10,000.00	€20,000.00	€30,000.00
WTIV	Per day	€100,000.00	€200,000.00	€300,000.00

Note. "Operation" and "Unit" show the operation and corresponding unit respectively. The next three columns show these costs for a "10 MW," "15 MW" and "20 MW" size turbine. Similarly "Vessel" indicates the vessel type and costs for increasing vessel sizes.

Table 5 summarizes the costs based on estimates from literature and company data. However, these are difficult to verify due to confidentiality. Regardless, experts in the field have deemed that these values are in the right order of magnitude.

In practice, port capacity is reserved such that 50 % of the project turbines can be stored, which ensures components are always available. Fig. 6 visualizes the costs for each of the reference projects per year for this port capacity.

This shows that the WTIV costs comprise at least 50 % and up to 75 % of the total costs. Moreover, it should be noted that aspects such as port capacity and the vessel fleet are fixed for a given project once it has started. Therefore, the only method to reduce costs is to minimize the project duration, as then both port capacity and the vessels can be rented for a shorter period. Therefore, it is sufficient to maximize the installation rate for a given project, as costs will be minimized as a result. The installation rate, I_{rate}, is defined as number of installed wind turbines per day, and calculated by dividing the number of installed turbines by the project duration in days.

4.2. Verification of the Markov model

The Markov model is calibrated on ERA5 hourly data from 1979 to 2000, see Hersbach et al. (2020) for further details on the dataset. However, N and ρ still have to be tuned for the best forecasting accuracy. The forecasting period is set to two weeks.

Based on Fig. 7a, there is an optimum for ρ around 0.5. Additionally, based on Fig. 7, the forecast accuracy does not significantly improve for a higher number of simulations than 10. Therefore, the number of simulations is set to 10 and rho to 0.5 for this paper. We find an average forecast accuracy of 72.92 % over a two-week forecasting horizon concerning weather windows. In general, it is difficult to compare the forecasting accuracy to regular weather forecasts. However, Pandit et al. (2020) have shown that Markov models perform well in determining the wind speed for offshore wind farms. Similarly, Rippel et al. (2019a) also find that a Markov approach performs well. Moreover, both emphasize the benefits of lack of training time and specific parameter optimization compared to other models. Therefore, we conclude that the Markov model is a suitable choice.

4.3. Experimental setup

The experimental setup is key to gaining relevant insights. Table 6 summarizes the four experiments, which ensure relevant insights can be derived. Per experiment, a full factorial approach is used, for all three reference projects and both shuttling and feedering, e.g. yielding $3 \times 3 \times 2 = 18$ combinations for the distance experiment. Table 7 shows the general parameter settings, which result in a runtime of five minutes per combination.

Firstly, we perform an experiment related to the distance between the marshalling port and the OWF to see how this affects the installation rate. Secondly, we examine if larger vessels make the installation process more efficient as, theoretically, less time is spent on sailing. Thirdly, we analyze how different weather conditions impact the installation rates of both strategies. Lastly, we perform an experiment related to buffer size to check if, with sufficient starting inventory, the WTIV can be used as efficiently as possible, as components are always available. It should be noted that the efficiency is measured in terms of the installation rate, I_{rate}, for all experiments. The installation rate is defined as the number of installed wind turbines per day and calculated by dividing the number of installed turbines by the project duration in days.

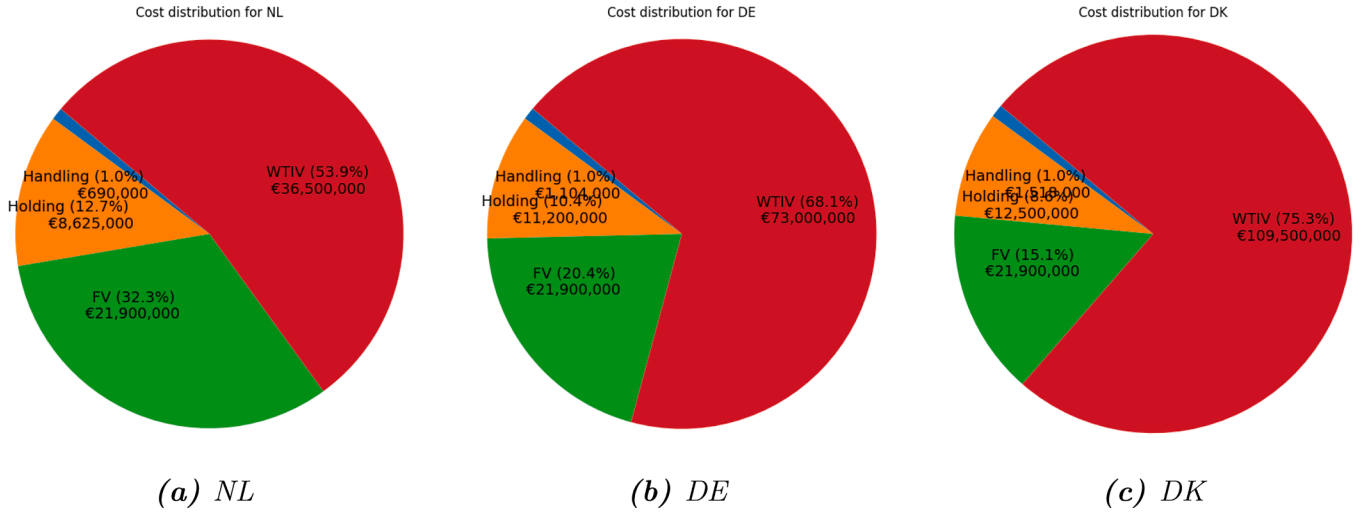

Fig. 6. Visualisation of handling (blue), holding (orange), FV (green) and WTIV (red) costs.

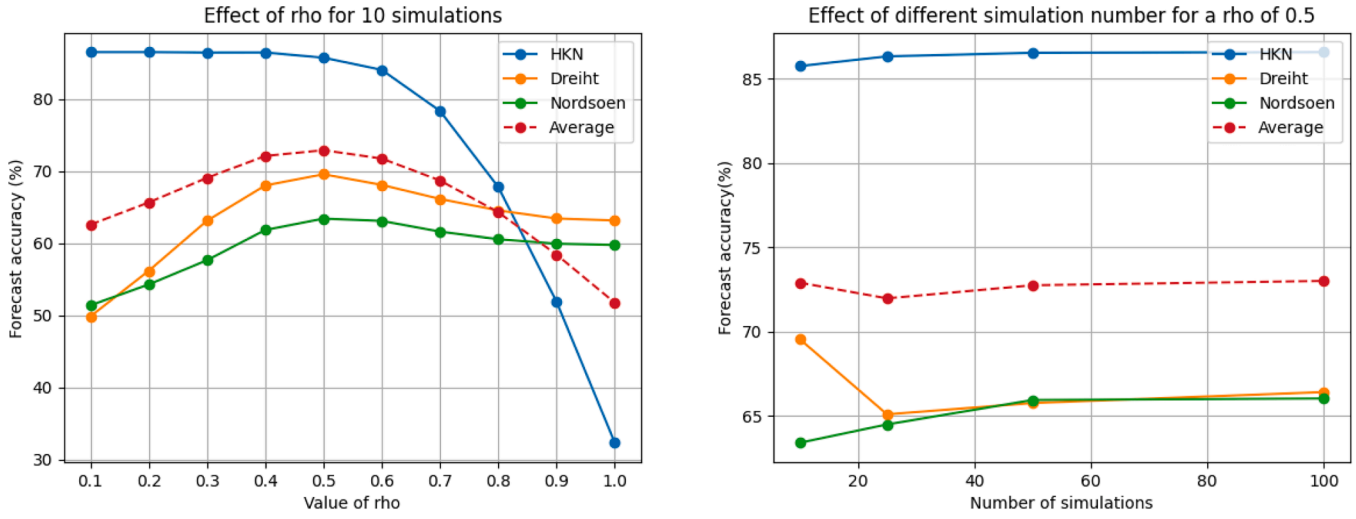

(a) Effect of different ρ values if $N = 10$ *(b) Effect of increasing N if $\rho = 0.5$*

Fig. 7. Effects of ρ and N on the forecast accuracy.

Table 6
Overview of the experimental setup.

Distance	Values
Marshalling port	[Eemshaven, Esbjerg, Hull]
Vessel size	**Values**
WTIV	[Small, Medium, Large]
FV	[Small, Medium, Large]
Weather	**Values**
Simulation year	[2003, 2015, 2023]
Alpha	[1, 1.2, 1.5]
Weather forecast	[Markov, Accurate]
Buffer size	**Values**
Production time (h)	[54, 81, 162]
Starting inventory (%)	[0–100, $\delta = 10$]

Table 7
Parameter settings.

Parameter	Value
Buffer size	50 %
Production time (h)	54
Weather model	Markov
N	10
ρ	0.5
α	1
Forecast horizon (h)	342
Time unit (h)	9
Optimization model	Greedy
Greedy its	25
Sim start	01-04-2022
Sim end	01-01-2024

4.4. Distance experiment

In this section, the results of the distance experiments are discussed. Table 8 shows the installation rates for the three projects, where the marshalling port location is varied. The highest installation rate is highlighted in bold per project, which results in the shortest project duration.

Based on Table 8, on average, for the standard port configuration of each project from Section 4.1, feedering has a 9.2 % higher installation rate than shuttling, whilst the required port capacity is similar. The port capacity for feedering is the sum of the three manufacturing ports, and for shuttling it is the capacity at the marshalling port. It should be noted that, generally, the best strategy in terms of installation rate also minimizes the required port capacity.

For both DE and NL, feedering is the best strategy according to Table 8, regardless of the marshalling port location for shuttling. For NL, the installation rate of feedering is at least 29.2 % higher than shuttling, whereas, for DE, this is 3.8 %. This is interesting as Eemshaven is located 100 km away from the OWF for DE, which is only a five-hour sail. Whereas, for feedering, the furthest manufacturing port lies almost 500 km away, which is a 40-h round trip. An explanation could be that this distance also has to be travelled to transport components to Eemshaven, but then the WTIV also has to travel back and forth to the port, adding extra time to the installation process and thus reducing efficiency. Feedering reduces project duration by two weeks for DE and almost two months for NL.

However, if the distance between the manufacturing ports and OWF becomes large, shuttling becomes more attractive, as is the case for DK in Table 8. Shuttling from Esbjerg is 12.9 % more efficient than feedering, saving almost 6 weeks in project duration. A big consideration still is that feedering requires no marshalling port at all. Interestingly, marshalling from Eemshaven or Hull, which are both located closer to the furthest manufacturing port, performs quite similarly to feedering, possibly due to the large distances between the marshalling port and OWF. This shows that if no marshalling port is available near the OWF, feedering can serve as a viable alternative, even if the distance between the manufacturing ports and OWF is over 1500 km.

These findings are in line with Oelker et al. (2018), who also find that if the distance between the OWF and the marshalling port is too large, shuttling becomes more attractive. It should be noted that Oelker et al. (2018) only tested a 4 and 7 h sailing time, whereas in this report, much larger sailing times, up to 60 h, are considered. Also, the difference in installation rate can not only be attributed to the distances. Both DE and DK face more challenging weather conditions than NL, which could also play a role. Fig. 8 shows the installed turbines for each project over time.

What can be observed is that installation under more difficult weather conditions, i.e. Fig. 8b and c, follows a sort of S-curve. This indicates that fewer turbines can be installed during the winter, where generally worse weather conditions occur. On the other hand, during the summer months, weather conditions are generally better, thus resulting in a higher installation rate. Since each project starts in April with an initial buffer of 50 %, each project starts with a high installation rate, but for both DE and DK, it is visible that after September, the

Table 8
Overview of the number of installed wind turbines per project and port setup. The first column shows the project. The second and third columns show the strategy and marshalling port. The fourth and fifth columns show the distance between the OWF and marshalling port and the furthest manufacturing port to the OWF (feeder) or marshalling port (shuttle). The last three columns show the required port capacity, project duration, and installation rate, respectively.

Project	Strategy	Marshalling	D_{Mars} (km)	$D^{\max}_{Manu}$ (km)	Cap (ha)	Dur (d)	I_{rate}
NL	**Feeder**	**–**	**–**	**381.97**	**8.5**	**202.00**	**0.3416**
NL	Shuttle	Eemshaven	307.76	343.06	9.5	261.00	0.2644
NL	Shuttle	Esbjerg	500.09	203.69	9.95	283.00	0.2438
NL	Shuttle	Hull	366.08	437.98	9.87	280.00	0.2464
DE	**Feeder**	**–**	**–**	**469.28**	**13.02**	**391.00**	**0.1637**
DE	Shuttle	Eemshaven	103.96	543.26	14.56	406.00	0.1576
DE	Shuttle	Esbjerg	274.31	158.47	14.49	428.00	0.1495
DE	Shuttle	Hull	447.98	638.18	14.91	420.00	0.1524
DK	Feeder	–	–	1513.68	16.5	352.00	0.1420
DK	Shuttle	Eemshaven	416.18	1402.72	14.7	364.00	0.1374
DK	**Shuttle**	**Esbjerg**	**75.18**	**1515.03**	**13.5**	**312.00**	**0.1603**
DK	Shuttle	Hull	648.79	1351.03	14.1	343.00	0.1458

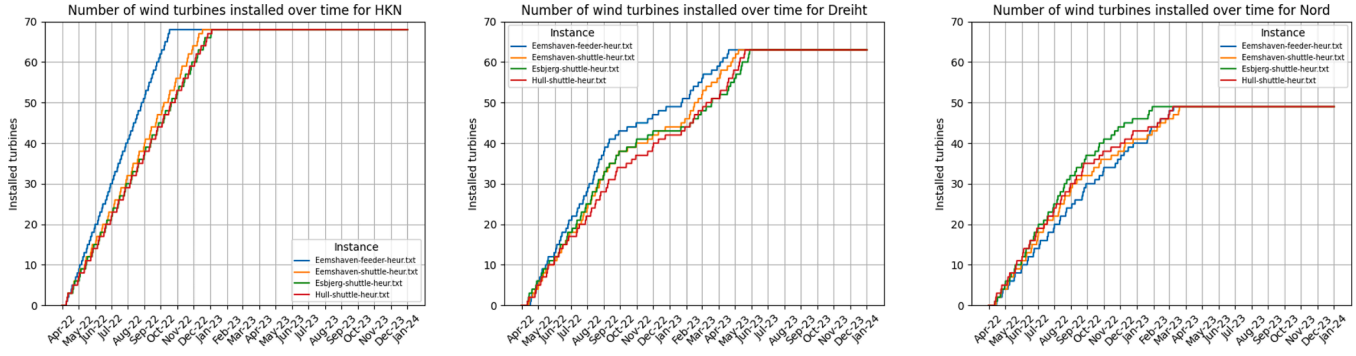

(a) NL *(b) DE* *(c) DK*

Fig. 8. Visualisation of installed wind turbines over time per project.

installation rate drops significantly up to March. Interestingly enough, both Fig. 8 and Table 8 imply that weather conditions are not the limiting factor in feedering. For DE and DK, which both face much more difficult weather than NL, feedering is still a feasible approach. The experiments in Section 4.6 further show that feedering is less weather-dependent than shuttling.

4.5. Vessel size experiment

In this section, the effects of the size of the FVs and WTIV are analyzed. Table 9 shows the numerical results of this experiment, averaged over the three projects, in terms of the installation rate. Let us consider the first three rows of Table 9, where the feeder vessels are small, and only the size of the installation vessel differs. It should first be observed that shuttling is 10–20 % more efficient than feedering. For shuttling, it can be observed that the installation rate generally increases for a larger WTIV. Despite the increasing size of the installation vessel, the installation rate barely changes for feedering. This could indicate that the small feeder vessels are restricting the installation rate. For feedering it is even restricting certain projects so much that they can not be finished by 2024 since the number of installed turbines is lower than 61. For shuttling, every project is finished by 2024. This shows that if the fleet of FVs is too small, having a marshalling port speeds up the projects significantly, as the components can get consolidated there and FVs do not have to wait for transshipment offshore.

Let us consider the next three rows, where the feeder vessel size is set to medium, the same size used for all other experiments. Interestingly, feedering now outperforms shuttling, which does confirm that the small FVs were limiting for feedering. For shuttling, the installation rate does not change significantly compared to the small FVs, which shows the small FVs were not limiting. Again, the installation rate for shuttling generally increases for a larger WTIV, but this increase is much larger for feedering, however. Using a large WTIV instead of a small WTIV increases the installation rate by 14.7 % and reduces project duration by 7 weeks on average. This effect likely occurs since larger WTIVs can serve as an offshore buffer, thus being able to install whilst the FVs are collecting components.

Finally for the last three rows with the largest feeder vessels, we notice that for shuttling the installation rate once again does not change significantly. For feedering, however, installation rates are at least 4.5 % higher than for medium feeder vessels. Additionally, larger WTIVs now drastically increase the installation rate. Using large instead of small WTIVs increases the installation rate by 19.9 % for feedering. Reducing project duration by over 8 weeks and by a further month compared to medium feeder vessels. This results in feedering being almost 25 % more efficient than shuttling.

Overall, these results are very interesting because, for shuttling, the size of the feeder vessels to transport components from the manufacturing to the marshalling port does not matter, and the size of the installation vessel only has a marginal effect on the installation rate. For feedering, the feeder vessels must be sufficiently large; otherwise, the installation rate gets restricted significantly. However, if the feeder vessels are sufficiently large, the installation rate is up to 25 % higher than for shuttling, resulting in 10 weeks shorter projects on average. So as long as the feeder vessels are sufficiently large, feedering generally utilizes the WTIV more efficiently than shuttling.

Table 9
Effect of WTIV and FV size on installation rate, averaged over the projects. The first two columns indicate the WTIV and FV used. The next four columns indicate the strategy used, number of installed wind turbines, duration and installation rate. First for feedering, then for shuttling. Results are averaged over the three projects.

WTIV	FV	Strat	I_{WT}	Dur (d)	I_{rate}	Strat	I_{WT}	Dur (d)	I_{rate}
Small	Small	Shuttle	61.00	382.33	0.1595	Feeder	60.00	426.67	0.1406
Medium	Small	Shuttle	61.00	351.00	0.1738	Feeder	60.67	424.67	0.1429
Large	Small	Shuttle	61.00	359.67	0.1696	Feeder	61.00	416.33	0.1465
Small	Medium	Shuttle	61.00	374.00	0.1631	Feeder	61.00	363.33	0.1679
Medium	Medium	Shuttle	61.00	356.67	0.1710	Feeder	61.00	325.00	0.1877
Large	Medium	Shuttle	61.00	363.33	0.1679	Feeder	61.00	316.67	0.1926
Small	Large	Shuttle	61.00	376.67	0.1619	Feeder	61.00	344.67	0.1770
Medium	Large	Shuttle	61.00	354.33	0.1722	Feeder	61.00	311.00	0.1961
Large	Large	Shuttle	61.00	357.67	0.1705	Feeder	61.00	287.33	0.2123

Table 10
Effects of weather windows and simulation year on installation rate. The first two columns indicate the simulation year and α factor. The next four columns indicate the strategy used, total number of installed wind turbines, duration and installation rate. First for feedering, then for shuttling. Results are averaged over the three projects.

Year	α	Strat	$I_{rate}^{forecast}$	$I_{rate}^{accurate}$	Diff (%)	Strat	$I_{rate}^{forecast}$	$I_{rate}^{accurate}$	Diff (%)
2003	1	Shuttle	0.1900	0.1959	3.12	Feeder	0.2133	0.2240	5.02
2003	1.2	Shuttle	0.1511	0.1706	12.96	Feeder	0.1551	0.1631	5.11
2003	1.5	Shuttle	0.1289	0.1563	21.28	Feeder	0.1327	0.1577	18.79
2015	1	Shuttle	0.1594	0.1796	12.70	Feeder	0.1785	0.1826	2.31
2015	1.2	Shuttle	0.1327	0.1393	4.94	Feeder	0.1329	0.1416	6.57
2015	1.5	Shuttle	0.1205	0.1366	13.39	Feeder	0.1195	0.1390	16.26
2023	1	Shuttle	0.1842	0.1918	4.13	Feeder	0.1909	0.1969	3.17
2023	1.2	Shuttle	0.1370	0.1454	6.14	Feeder	0.1452	0.1496	2.97
2023	1.5	Shuttle	0.1288	0.1438	11.69	Feeder	0.1287	0.1442	12.12

4.6. Weather experiment

In this section, the results of different years of simulation and α safety factors for durations are discussed. 2003 is a good weather year, 2015 a bad weather year and 2023 an average year based on the historical weather data. Table 10 shows the effect on the installation rate for simulating in these years averaged over the three projects. Additionally, the value of 100 % accurate forecasts is also tested. Each simulation is performed for the full year, which means projects might not finish and start in January of the respective year.

Based on the $I_{rate}^{forecast}$ from Table 10, both feedering and shuttling performed better in 2003 than in the other years due to the better weather conditions. Especially feedering performs over 10 % better than in 2023 and almost 20 % better than in 2015 for $\alpha = 1$. For shuttling this is only 3 % for 2023 and almost 20 % for 2015. Moreover, even in 2015, feedering outperforms shuttling. This is surprising as it would be expected that for worse weather conditions it becomes more difficult to transship and install offshore. This could also be explained because for shuttling the WTIV is missing installation windows during the sailing, whereas for feedering these windows can be utilized. This shows that the weather conditions do significantly impact the installation rate, but feedering suffers less from worse weather conditions.

Regardless of the installation year or forecast quality, it can be observed that the number of installed wind turbines decreases drastically for an increasing α factor. Moreover, from Table 10 it seems that the installation rates of shuttling and feedering start to converge for larger values of α. This is the case for both the Markov and accurate forecasts, but the installation rate is significantly higher for the accurate forecasts. This indicates that shuttling and feedering make use of the same weather windows and this is the limiting factor on the installation rate.

Table 10 also shows that 100 % accurate forecasts improves the installation rate, $I_{rate}^{accurate}$, anywhere between 2.31 % and 21.28 % compared to $I_{rate}^{forecast}$, especially for higher values of α. This is not surprising, as longer weather windows are more difficult to forecast. For $\alpha = 1$ a 5.05 % average increase in installation rate is observed. This means the added value of increasing the forecast accuracy is mainly interesting for larger values of α, as for $\alpha = 1.5$ the average increase is 15.59 %. Interestingly, shuttling seems to benefit more from accurate forecasts, likely since the forecast has a large influence on when the WTIV sails out to install. However, even with 100 % accurate forecasts, feedering remains more efficient than shuttling, be it less significant. This shows that, regardless of the forecast accuracy and simulation year, feedering is generally more efficient than shuttling.

4.7. Initial buffer experiment

In practice, projects do not start with zero initial inventory. Instead, first, a buffer of 50 %, deemed as B_{trad}, is built up such that installation is not limited by component availability as there are large lead times on components (CEIF, 2022). Predictably, as the initial buffer gets larger, the required port capacity also gets larger. Fig. 9 illustrates the maximum port usage for the different buffer sizes. For feedering this is the total capacity summed over the three manufacturing ports.

Two trends are observable from Fig. 9. First, the required port capacity increases linearly for larger initial buffers, but at different slopes, depending on the production time. This indicates that the initial buffer size is also the largest inventory that is in the port at any point. Second, up to 20 % buffer, this trend does not hold. This makes sense as 0 % buffer port capacity is still required, as components still have to be stored. The same holds for 10 % and 20 % buffer. This means that this port capacity has to be reserved regardless, thus it might as well be filled with a 20 % initial buffer as this increases the installation rate. In general, it can be noted that the required port capacity is a direct result of the production time and initial buffer size and does not depend on the strategy, as Fig. 9 shows similar values for both shuttling and feedering. Fig. 10 visualizes the results of this experiment for different production rates and initial buffer sizes on the installation rate.

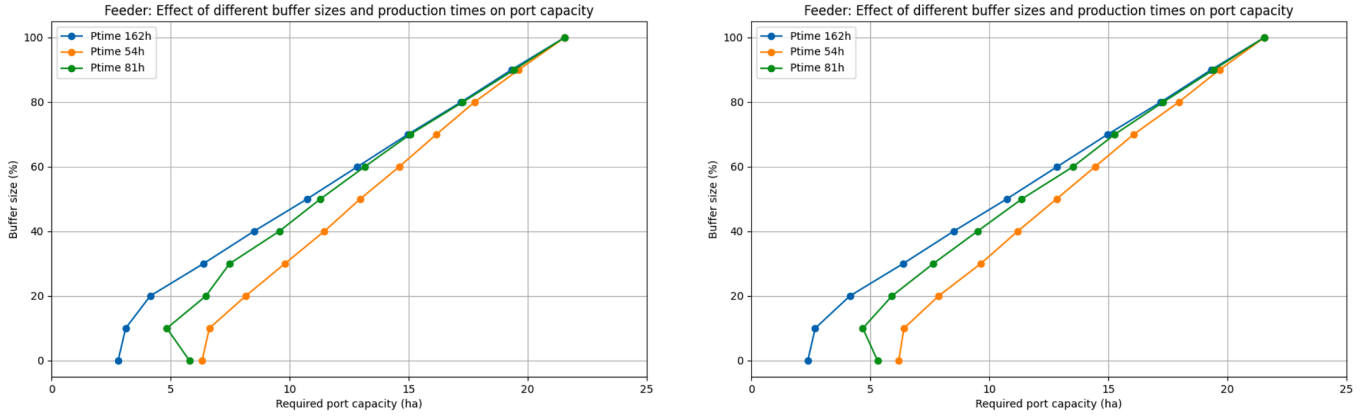

(a) Shuttle *(b) Feeder*

Fig. 9. Maximum port capacity used vs initial buffer size for different production times.

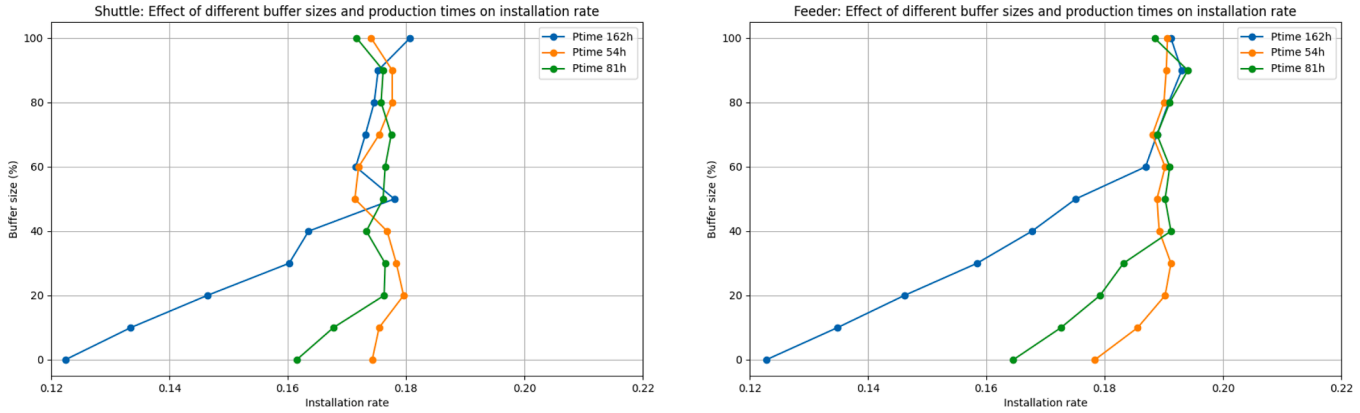

(a) Shuttle *(b) Feeder*

Fig. 10. Average installation rate vs initial buffer size for different production times.

Fig. 10 shows two interesting trends. First, if an insufficient initial buffer is available, the installation rate gets restricted by the production time, indicated by the linear installation rate. Second, feedering requires larger buffers than shuttling, due to the higher installation rate, indicated by the line continuing longer than for shuttling. This shows there is a direct relation between the installation rate, initial buffer size and production time.

There also seems to be some noise or clutter in Fig. 10, as there are variations in the installation rate, even if sufficient initial buffer is available. This is caused by the averaging over the three projects. As observed from Fig. 10, the initial buffer size seems to depend on the production time and installation rate. A standard buffer size formula would be:

$$B_{std} = 1 - \frac{P_{rate}}{I_{rate}} \tag{21}$$

where B_{std} is the fraction of the wind turbines required as initial buffer size and P_{rate} and I_{rate} are the production and unrestricted installation rate respectively. The unit of P_{rate} and I_{rate} does not matter as long as they are the same. This formula is based on the cycle inventory formula, but instead of calculating the average inventory, we are trying to calculate the maximum inventory needed to not run out of components, so we do not divide by 2. This is expressed via B, which indicates which fraction of the total turbines should be stored initially.

Assuming that the production rate is lower than the installation rate, otherwise, no initial buffer is required. Based on the results, the average unrestricted installation rate for feedering is roughly 0.19 turbines per day and for shuttling this is 0.17. 162 h of production time results in a production rate of 0.15. For feedering this would mean an initial buffer of 20 % and for shuttling 10 % of the total turbines. However, based on Fig. 10 this is not sufficient for both shuttling and feedering.

The first thing to consider is that Eq. (21) applies to fully linear processes where the production and installation rates are constant over time. For this problem that is not the case as the installation rate differs over time due to the weather conditions. Moreover, the installation rate also takes into account the time it takes from production to installation. So the manufacturing, transportation and storage times are also included, which might cause Eq. (21) to not work as installation time also covers non-installation-related processes.

Therefore, a simple formula to calculate the so-called unrestricted installation time is proposed, which can be used in (21). The unrestricted installation time ($I*_{time}$) refers to the theoretical installation time if components are always available and can be calculated as:

$$I*_{time}^{Shuttle} = T^{Sailing} + T^{Loading} + \frac{T^{Install}}{W^2} \tag{22}$$

$$I*_{time}^{Feeder} = \frac{T^{Trans} + T^{Install}}{W^2} \tag{23}$$

where $T^{Sailing}$, $T^{Loading}$, T^{Trans}, and $T^{Install}$ indicate the time required for sailing, loading, transshipping, and installing per turbine, respectively. W indicates during which fraction of the year installation is possible. The weather-dependent activities are then divided by W^2 to account for the time when these activities are not possible, the square ensures a penalty for overlapping installation windows. I.e. during good weather conditions, installation can only happen after the previous installation is finished. This results in an new proposed buffer size formula, where

Table 11
Overview of predicted buffer sizes and actual buffer size required. For each project, production time and strategy, the predicted buffer size according to practice B_{trad} and the proposed formula B_{prop} is shown, bold highlights which is closest to the actual required buffer B_{act}.

Project	P_{time} (h)	$B^{shuttle}_{trad}$	$B^{shuttle}_{prop}$	$B^{shuttle}_{act}$	B^{feeder}_{trad}	B^{feeder}_{prop}	B^{feeder}_{act}
NL	54.00	0.50	**0.05**	0.10	0.50	**0.25**	0.20
NL	81.00	0.50	**0.37**	0.20	**0.50**	**0.50**	0.40
NL	162.00	0.50	**0.68**	0.60	0.50	**0.75**	0.70
DE	54.00	0.50	**0.00**	0.00	0.50	**0.00**	0.10
DE	81.00	0.50	**0.00**	0.00	0.50	**0.00**	0.10
DE	162.00	0.50	**0.29**	0.20	0.50	**0.35**	0.40
DK	54.00	0.50	**0.00**	0.00	0.50	**0.00**	0.00
DK	81.00	0.50	**0.00**	0.20	0.50	**0.00**	0.00
DK	162.00	0.50	**0.28**	0.20	0.50	**0.41**	0.20

we convert the $I*_{time}$ to $I*_{rate}$ such that it has the same unit as P_{rate}:

$$B_{prop} = 1 - \frac{P_{rate}}{I*_{rate}} \tag{24}$$

Table 11 shows the predicted buffer size based on B_{prop}, the traditional 50 % buffer approach, B_{trad}, and the actual required buffer size, B_{act}. The closest buffer, in terms of absolute deviation, to B_{act} is highlighted in bold.

Table 11 illustrates that for all three project and production rates B_{prop} is much closer to B_{act} for both shuttling and feedering. There is only one case where the same buffer size is predicted by B_{trad}, which is likely a result of chance. On average, the traditional approach deviates 0.33 from B_{act} ($MSE = 0.13$), whereas the B_{prop} approach only deviates 0.07 on average ($MSE = 0.01$). This shows the use of the traditional approach should be reconsidered as it is much too naive and robust. Therefore, the initial buffer should be calculated depending on project-dependent characteristics, as this can increase the installation rate or reduce the required port capacity depending on the project.

5. Discussion

Offshore wind expansion faces three challenges: (i) limited installation vessel fleet, (ii) limited port capacity, and (iii) operational susceptibility to weather conditions. Each challenge and the insights gained regarding this challenge are elaborated on, based on the results from the computational experiments.

1. **Limited fleet of wind turbine installation vessels**
   Due to the limited WTIV fleet, the installation rate has to be increased significantly to meet the 2030 climate ambitions. By only starting the installation process with a certain buffer already available, the installation rate increases significantly for both shuttling and feedering, as now components are readily available for installation.

   Feedering generally increases the installation rate and reduces project duration by 9.21 % compared to shuttling. This shortens project duration by 29 days on average, which could save millions. Additionally, feedering is less dependent on the quality of the weather forecast and weather conditions in general, so is also more robust than shuttling.

   Shuttling starts being more efficient than feedering if the manufacturing ports are located more than 1000 km from the OWF and the marshalling port lies within 500 km of the OWF. However, if manufacturing ports lie within roughly 500 km of the OWF, feedering is more effective. Additionally, if the size of the feeder vessels is too small, shuttling also becomes more efficient than feedering.
2. **Limited port capacity**
   Results show that production rates have a significant impact on the required port capacity. If the production rate is 54 instead of 81 h, a limited amount of port capacity is needed as just-in-time logistics can be used. However, if the production time is 162 h per component, buffers of up to 70 % of the project size could be required. This translates to roughly 20ha of storage area for a 1 GW project, which might not be available in the future.

   Results also show that the required port capacity is directly related to the production time and initial buffer. Thus calculating the required initial buffer accurately will also result in the lowest amount of reserved port capacity, whilst optimizing the installation rate. The proposed formula (24) predicts the required buffer size much more closely than the traditional 50 % for all projects and production times. Using the 50 % is too naive and results in a significant over- or under-utilization of the port. This results in roughly 8ha against 2ha of unnecessarily reserved port capacity respectively for a 1 GW project, which shows more accurate initial buffer calculations can save hectares of required port capacity.

   Since shuttling generally has a lower installation rate than feedering, it also requires less initial buffer. So if port capacity is an issue, shuttling should be considered, but this does result in a longer project duration. So whilst it might help for port capacity, it could increase the pressure on the WTIV fleet.
3. **Dependence on weather conditions**
   Weather conditions play a significant role in the installation rate and project duration of offshore wind projects. Feedering, on average, performs better than shuttling in any simulated year for the nominal weather window, i.e. $\alpha = 1$. Compared to an average year, the installation rate increases by 3.1 and 11.7 % for shuttling and feedering respectively in a good year. In a bad year, installation rates decrease by 13.5 and 6.5 % respectively. This means that feedering benefits more from good weather and is affected less by worse weather.

   Moreover, increasing the accuracy of the weather forecast can increase the installation rate significantly. Especially for higher values of α, a more accurate weather forecast can increase the installation rate by anywhere between 11.69 % and 21.28 %. For $\alpha = 1$ this effect is less pronounced, as installation rates increase by 5.05 % on average. Additionally, shuttling benefits much more from higher-quality forecasts, as this likely allows for a better choice of when to sail out for installation from the port.

These findings are directly in line with Oelker et al. (2018), who also find that distance to the offshore wind farm and vessel capacity and number of feeder vessels in their study, respectively, are the limiting factors on feedering.

There are some limitations to the model. The key assumptions are that vessels can remain offshore indefinitely, sailing is not considered weather-dependent, and port logistics are considered on an aggregate scale. Whilst these limitations should be considered when studying the results, the motivation, verification, and validation show that the impact is limited and that the results are representative and realistic.

For future research, weather forecasting could be further developed, as more accurate forecasts result in higher installation rates. It would also be interesting to link the approach used in this paper directly to industry guidelines, i.e., DNVGL-ST-N001, which specifies rules for forecasting and operational limits. We define α as a general safety factor for the forecasts, which is also used in the industry guidelines. DNVGL-ST-N001 specifies a more detailed approach to determine when operations are allowed. However, according to industry experts supporting this work, the proposed approach does capture the essence of the operational limits, and the results were validated during the analysis. For future research, the application of the whole DNVGL-ST-N001 standard is interesting and could be integrated in the proposed decision support framework.

Alternatively, (meta)heuristics could be used to handle more supply chain aspects, such as port congestion, refueling, or recrewing. It could also be insightful if a practical test case were performed using feedering to validate the results of this paper and explore any practical bottlenecks.

6. Conclusion

In this study, we propose a rolling horizon simulation framework for the evaluation and optimization of offshore wind farm logistics. The framework uses a Markov weather forecasting model and optimization heuristic, which allows us to quickly solve the MILP within the rolling horizon loop.

We find that the locations of manufacturing ports in combination with the production rate of components should be considered as this has a significant impact on the installation rate and which initial buffer is required. The 50 % initial buffer rule used in practice is much too naive and project-dependent characteristics should be considered, as this predicts the required buffer size much more accurately. Shuttling only becomes more efficient than feedering if the manufacturing ports are located far away from the offshore wind farm or if the feeder vessels are too small. In all other circumstances, feedering outperforms shuttling and is also less weather-dependent according to our experiments. Therefore, the industry should start exploring feedering as a feasible strategy to increase the installation rate and meet the 2030 climate goals, whilst keeping into account the effects of manufacturing ports.

Declaration of competing interest

The authors declare that they have no known competing financial interests or personal relationships that could have appeared to influence the work reported in this paper.

CRediT authorship contribution statement

Tenzin Frijlink: Writing – review & editing, Writing – original draft, Validation, Software, Methodology, Investigation, Formal analysis, Data curation, Conceptualization; **Stefano Fazi:** Writing – review & editing, Writing – original draft, Validation, Supervision, Investigation, Conceptualization; **Lori Tavasszy:** Writing – review & editing, Writing – original draft, Supervision, Investigation, Conceptualization; **Mark Duinkerken:** Writing – review & editing, Writing – original draft, Supervision, Investigation, Conceptualization; **Leon Lammers:** Writing – review & editing, Validation, Supervision, Software, Investigation, Data curation.

References

Barlow, E., Öztürk, D.T., Revie, M., Akartunali, K., Day, A.H., Boulougouris, E., 2018. A mixed-method optimisation and simulation framework for supporting logistical decisions during offshore wind farm installations. Eur. J. Oper. Res. 264, 894–906. https://doi.org/10.1016/j.ejor.2017.05.043

Barlow, E., Tezcaner Öztürk, D., Revie, M., Boulougouris, E., Day, A.H., Akartunali, K., 2015. Exploring the impact of innovative developments to the installation process for an offshore wind farm. Ocean Eng. 109, 623–634. https://doi.org/10.1016/J.OCEANENG.2015.09.047

Beinke, T., Ait Alla, A., Freitag, M., 2017. Resource sharing in the logistics of the offshore wind farm installation process based on a simulation study.Int. J. e-Navig. Marit. Econ. 7, 42–54. https://doi.org/10.1016/J.ENAVI.2017.06.005

uit het Broek, M. A.J., Veldman, J., Fazi, S., Greijdanus, R., 2019. Evaluating resource sharing for offshore wind farm maintenance: the case of jack-up vessels. Renew. Sustain. Energy Rev. 109, 619–632.

CEIF, 2022. Ensuring the supply chain can deliver an expansion of offshore wind in Europe Recommendations to NSEC Governments-October 2022. Technical Report.

Díaz, H., Guedes Soares, C., 2020. Review of the current status, technology and future trends of offshore wind farms. Ocean Eng. 209, 107381. https://doi.org/10.1016/J.OCEANENG.2020.107381

Fazi, S., Fransoo, J.C., Van Woensel, T., 2015. A decision support system tool for the transportation by barge of import containers: a case study. Decis. Support Syst. 79, 33–45.

Gonzalez, M. O.A., Nascimento, G., Jones, D., Akbari, N., Santiso, A., Melo, D., Vasconcelos, R., Godeiro, M., Nogueira, L., Almeida, M., Oprime, P., 2024. Logistic decisions in the installation of offshore wind farms: a conceptual framework. Energies 17, 6004. https://doi.org/10.3390/EN17236004/S1

H-Blix, 2022. H-BLIX Offshore wind vessel availability until 2030: Baltic Sea and Polish perspective-Offshore wind vessel availability until 2030: Baltic Sea and Polish perspective Final Report https://windeurope.org/wp-content/uploads/files/policy/topics/offshore/Offshore-wind-vessel-avaiability-until-2030-report-june-2022.pdf.

Hersbach, H., Bell, B., Berrisford, P., Hirahara, S., Horanyi, A., Munoz-Sabater, J., Nicolas, J., Peubey, C., Radu, R., Schepers, D., Simmons, A., Soci, C., Abdalla, S., Abellan, X., Balsamo, G., Bechtold, P., Biavati, G., Bidlot, J., Bonavita, M., De Chiara, G., Dahlgren, P., Dee, D., Diamantakis, M., Dragani, R., Flemming, J., Forbes, R., Fuentes, M., Geer, A., Haimberger, L., Healy, S., Hogan, R.J., Holm, E., Janiskova, M., Keeley, S., Laloyaux, P., Lopez, P., Lupu, C., Radnoti, G., de Rosnay, P., Rozum, I., Vamborg, F., Villaume, S., Thepaut, J.N., 2020. The ERA5 global reanalysis. Q. J. R. Meteorolog. Soc. 146, 1999–2049. https://doi.org/10.1002/QJ.3803

Hong, S., McMorland, J., Zhang, H., Collu, M., Halse, K.H., 2024. Floating offshore wind farm installation, challenges and opportunities: a comprehensive survey. Ocean Eng. 304, 117793.

Hrouga, M., Bostel, N., 2021. Supply chain planning of off-Shores winds farms operations: a review. Lect. Notes Mech. Eng., 372–387. https://doi.org/10.1007/978-3-030-62199-5_33

Irawan, C.A., Jones, D., Ouelhadj, D., 2017. Bi-objective optimisation model for installation scheduling in offshore wind farms. Comput. Oper. Res. 78, 393–407. https://doi.org/10.1016/J.COR.2015.09.010

Lerche, J., Lindhard, S., Enevoldsen, P., Velaayudan, A., Teizer, J., Neve, H.H., Wandahl, S., 2022. What can be learned from variability in offshore wind projects. Energy Strategy Rev. 39, 100794. https://doi.org/10.1016/J.ESR.2021.100794

Makowski, C., 2023. scgraph: Supply chain graph package for Python. https://pypi.org/project/scgraph/.

NSEC, 2023. North Seas offshore wind port study 2030–2050—Final report. Technical Report.

Oelker, S., Ait-Alla, A., Lütjen, M., Lewandowski, M., Freitag, M., Thoben, K.-D., 2018. A simulation study of feeder-based installation concepts for offshore wind farms. In: Proceedings of the Twenty-eighth (2018) International Ocean and Polar Engineering Conference Sapporo, Japan. OnePetro. https://onepetro.org/ISOPEIOPEC/proceedings-abstract/ISOPE18/All-ISOPE18/ISOPE-I-18-332/20557.

Oelker, S., Alla, A.A., Büsing, S., Lütjen, M., Freitag, M., 2020. Simulative approach for the optimization of logistic processes in offshore ports. In: Proceedings of the Thirtieth (2020) International Ocean and Polar Engineering Conference Shanghai, China. https://www.researchgate.net/publication/344174221_Simulative_approach_for_the_optimization_of_logistic_processes_in_offshore_ports.

Pandit, R.K., Kolios, A., Infield, D., 2020. Data-driven weather forecasting models performance comparison for improving offshore wind turbine availability and maintenance. IET Renew. Power Gener. 14 (13), 2386–2394. https://doi.org/10.1049/IET-RPG.2019.0941

Paterson, J., Damico, F., Thies, P.R., Kurt, R.E., Harrison, G., 2018. Offshore wind installation vessels–a comparative assessment for UK offshore rounds 1 and 2. Ocean Eng. 148, 637–649.

Quandt, M., Beinke, T., Ait-Alla, A., Freitag, M., 2017. Simulation based investigation of the impact of information sharing on the offshore wind farm installation process. J. Renew. Energy 2017, 1–11. https://doi.org/10.1155/2017/8301316

Ren, Z., Jiang, Z., Skjetne, R., Gao, Z., 2018. Development and application of a simulator for offshore wind turbine blades installation. Ocean Eng. 166, 380–395.

Rippel, D., Jathe, N., Becker, M., Lütjen, M., Szczerbicka, H., Freitag, M., 2019a. A review on the planning problem for the installation of offshore wind farms. IFAC-PapersOnLine 52 (13), 1337–1342. https://doi.org/10.1016/J.IFACOL.2019.11.384

Rippel, D., Jathe, N., L'tjen, M., Freitag, M., 2019b. Evaluation of loading bay restrictions for the installation of offshore wind farms using a combination of mixed-integer linear programming and model predictive control. Appl. Sci. 9 (23), 5030. https://doi.org/10.3390/APP9235030

Ritchie, H., 2024. Weather forecasts have become much more accurate; we now need to make them available to everyone. Our World in Data https://ourworldindata.org/weather-forecasts.

Sarker, B.R., Faiz, T.I., 2017. Minimizing transportation and installation costs for turbines in offshore wind farms. Renew. Energy 101, 667–679. https://doi.org/10.1016/J.RENENE.2016.09.014

Scholz-Reiter, B., Karimi, H.R., Lütjen, M., Heger, J., Schweizer, A., 2011. Towards a Heuristic for Scheduling Offshore Installation Processes.

Scholz-Reiter, B., Lütjen, M., Heger, J., Schweizer Biba Bremer, A., 2010. Planning and control of logistics for offshore wind farms http://www.biba.uni-bremen.de.

Tian, B., Zhang, J., Demeulemeester, E., Chen, Z., Ali, H., 2023. Integrated resource-constrained project scheduling and material ordering problem considering storage space allocation. Comput. Ind. Eng. 185, 109608. https://doi.org/10.1016/J.CIE.2023.109608

Tjaberings, J., Fazi, S., Ursavas, E., 2022. Evaluating operational strategies for the installation of offshore wind turbine substructures. Renew. Sustain. Energy Rev. 170, 112951. https://doi.org/10.1016/J.RSER.2022.112951

Ursavas, E., 2017. A benders decomposition approach for solving the offshore wind farm installation planning at the North Sea. Eur. J. Oper. Res. 258 (2), 703–714. https://doi.org/10.1016/J.EJOR.2016.08.057

Vis, I. F.A., Ursavas, E., 2016. Assessment approaches to logistics for offshore wind energy installation. Sustain. Energy Technol. Assess. 14, 80–91. https://doi.org/10.1016/J.SETA.2016.02.001